HOKKAIDO UNIVERSITY

Title	Interannual variability in the magnitude and timing of the spring bloom in the Oyashio region
Author(s)	Okamoto, Suguru; Hirawake, Toru; Saitoh, Sei-Ichi
Citation	Deep Sea Research Part II: Topical Studies in Oceanography, 57(17-18), 1608-1617 https://doi.org/10.1016/j.dsr2.2010.03.005
Issue Date	2010-09
Doc URL	http://hdl.handle.net/2115/43804
Type	article (author version)
File Information	DSR2-57-17-18_1608-1617.pdf

Instructions for use

Hokkaido University Collection of Scholarly and Academic Papers : HUSCAP

Interannual variability in the magnitude and timing of the spring bloom in the Oyashio region

Suguru Okamoto*, Toru Hirawake and Sei-Ichi Saitoh

Affiliations:

Laboratory of Marine Bioresource and Environment Sensing, Graduate School of Fisheries Sciences, Hokkaido University, Hokkaido, 041-8611 Japan. (*oka@salmon.fish.hokudai.ac.jp)

Abstract:

Inter-annual variability in the magnitude and timing of the spring bloom was investigated for the Oyashio region (40 ˚-48 ˚N, 143 ˚E-152 ˚E) using 10 years (from 1998 to 2007) of satellite ocean color data. Geostrophic currents were examined using satellite altimeter data. Early spring blooms (> 1.5 mg m^{-3}) occurred in early April 2001 and late March 2002. The 2001 bloom continued for one month. Late blooms occurred from mid-May 1999, early June 2004 and late April 2006, continuing for about 1 month, 8 days and 16 days, respectively. A strong bloom (4.7 mg m^{-3}) also occurred in mid-April 1998; however, it terminated in early May. We classified the Oyashio region based on the pattern of temporal variation of Chl-*a* concentration from March to June. The spatio-temporal variability in Chl-*a* concentration during spring was different among years. The area where Chl-*a* concentration was highest in April was more extensive in 2001, 2002 and 2006 than usual. In 1999, the area where Chl-*a* concentration was highest in May was the widest among the 10 years. Mesoscale eddies and currents with high velocity were frequently observed in the area of high Chl-*a* concentration east of Hokkaido, advecting Coastal Oyashio Water of low salinity and low density into the oceanic region. That strengthened stratification in the surface layer. We suggest that this seaward transfer of coastal water could be one of the

important factors for phytoplankton distribution in two ways: (1) horizontal advection of water with high Chl-*a* concentration and (2) enhancement of stratification in the oceanic region.

Keywords: satellite data; spring bloom; Chl-*a* concentration; spatio-temporal variability; geostrophic current, Oyashio

1. Introduction

The Oyashio is a western boundary current that flows southwest along the southern Kuril Islands and southeast coast of Hokkaido and then circulates counterclockwise in the western North Pacific (Fig. 1). It carries cold water of reduced salinity to the western subarctic Pacific off Hokkaido (Kono, 1997). The Oyashio region has a nutrient-rich water mass, and it supports consumption of nitrate by phytoplankton with high efficiency (Taniguchi, 1999). The primary production is effectively transferred to higher trophic levels such as planktivorous pelagic fishes. The region supports a wide range of commercially important marine fishes (Sakurai, 2007).

In recent decades, the Oyashio ecosystem has shown significant changes in abundance and distribution of numerous species. Therefore, many studies about the ecosystem, from lower to higher trophic levels (phytoplankton, zooplankton, fishes), have been conducted (e.g., Kasai et al., 1997; Chiba et al., 2004; Sakurai, 2007). Spring phytoplankton blooms (e.g., Kasai et al., 1997; Saito et al., 2002) and their associated high primary productivity result in high zooplankton biomass, providing a rich food environment for fishes (Taniguchi, 1999; Sakurai, 2007). Abundant nutrients supplied to the surface layer by vertical mixing in wintertime have been suggested as one of the factors supporting the intense spring blooms (Kasai et al., 1997; Taniguchi, 1999). It has

been suggested recently that dissolved iron supplied from iron-rich intermediate waters to the surface also enables the spring phytoplankton bloom in the Oyashio region (Nishioka et al., 2007). Finally, stratification of the water column promotes the nutrient utilization by phytoplankton in the euphotic layer, and stratification is important for initiation of the spring bloom (Yoshimori et al., 1995; Kasai et al., 1997). The magnitude and duration of the spring bloom are different between the coastal and offshore regions because they can have different strengths of stratification and nutrient concentrations (Kasai et al., 1997). After 1998 when sea surface temperature was higher than before 1997, the spring bloom has been larger in magnitude and initiated earlier (Kasai and Ono, 2007). The Oyashio spring bloom is not always terminated by macronutrient depletion, and the magnitude and duration of the spring bloom in the region are in part controlled by the grazing pressure of zooplankton (Saito et al., 2002). Thus, many studies about the magnitude, timing and duration of the spring bloom have been conducted. However, as the sampling interval in these studies was about monthly and sampling stations were spatially limited (e.g., A-line in Fig. 1), it has yet to be understood whether the patterns observed in past studies extend over a larger area.

In this study, we present the spatio-temporal variability of Chl-*a* concentration during spring using satellite ocean color data from 1998 to 2007. Our objective is to

clarify the inter-annual variability in the magnitude and timing of the bloom in the Oyashio region. We also discuss the effect on the spring phytoplankton distribution of the horizontal advection of the Oyashio water mass into the offshore region by geostrophic currents.

2. Data and Methods

2.1. Satellite data validation

Sea-viewing Wide Field-of-view Sensor (SeaWiFS) data processed using the Ocean Color 4 version 4 (OC4v4) algorithm (O'Reilly et al, 1998, 2000) was used in this study. In the coastal region, satellite Chl-*a* concentration data using ocean color algorithms can be falsely interpreted due to light scattering by suspended particulates or absorbance by colored dissolved organic matter (e.g., Lee et al., 1994; Carder et al., 1989). Before analyzing Chl-*a* concentration data from SeaWiFS, we investigated its quality in the study area using the A-line dataset obtained from Fisheries Research Agency of Japan (FRA, 2009). We compared daily data from SeaWiFS with in-situ data during spring (March - June) from 1998 to 2007. SeaWiFS Chl-*a* concentration data were obtained from the NASA Goddard Space Flight Center's Distributed Active Archive Center (http://oceancolor.gsfc.nasa.gov/). These datasets have a spatial

resolution of about 9 km on an equidistant cylindrical projection.

2.2. Spatio-temporal variability of Chl-*a* concentration

The spatial and seasonal variability of Chl-*a* concentration in the Oyashio region (40 ˚-48 ˚N, 143 ˚-152 ˚E) from January 1998 to December 2007 was investigated using monthly and 8-day mean Chl-*a* concentration data from SeaWiFS. We calculated the 10-year mean of Chl-*a* concentration in each month and examined the seasonal variability of Chl-*a* concentration. We also extracted 8-day mean Chl-*a* concentration values averaged in each 3 × 3 pixel (27 × 27 km) area centered on the 13 stations along the A-line (from A1 to A13). Although the spring bloom in the Oyashio region has not been explicitly defined to investigate its timing, magnitude and duration previous studies, Kasai and Ono (2007) indicated that sea surface Chl-*a* concentration along the A-line in April and May from 1990 to 2003 was higher than about 1.5 mg m^{-3} and regarded that condition as a spring bloom. We therefore defined the spring bloom as in progress when Chl-*a* concentration is over 1.5 mg m^{-3}.

To investigate the variability of Chl-*a* distribution during spring, we analyzed monthly mean Chl-*a* concentration data from March to June, classifying sectors in the Oyashio region based on the temporal variation pattern of Chl-*a* concentration. We

applied an unsupervised classification, the Iterative Self-Organizing Data Analysis Technique (ISODATA), to the 10-year mean data from March to June. This method was also applied to the monthly mean Chl-*a* concentration data from March to June in each year. ISODATA clustering iteratively classifies the pixels in an image, redefines the criteria for each class, and classifies again, so that the spectral distance patterns in the data gradually emerge (ERDAS, 1999). The spectral distance was calculated as follows:

$$D = \sqrt{\sum_{i=1}^{n} (d_i - e_i)^2} \quad (1)$$

where D is the spectral distance, n is the number of bands (months), i is a particular band, and d_i and e_i are the data file values of pixels d and e, respectively, in band i. The ISODATA method uses minimum spectral distance of four bands (months) from March to June to assign each pixel to a cluster. On the first iteration of the ISODATA clustering, the means of 4 clusters were arbitrarily determined in this study. After each iteration, a new mean for each cluster was calculated, based on the actual distribution of the pixels in the cluster, instead of the initial arbitrary calculation. Then, these new means were used for defining clusters in the next iteration. The process continued until reaching a convergence threshold (95%), which was the maximum percentage of pixels whose cluster assignments were allowed to be unchanged between iterations. Eventually, the above 4 classes could be reclassified into 3 classes, for which the patterns of

seasonal variation in Chl-*a* concentration distinctly differed from one another. Those could be referred to variation in proportions of the three water types described in Kasai et al. (1997): Coastal, Oyashio, and Mixed waters. The ISODATA clustering enabled us to economically summarize the temporal variation of Chl-*a* concentration in each area and in each year.

2.3. Geostrophic currents

To estimate the geostrophic currents, we used weekly composite sea-level anomaly (SLA) data with a 1/3 degree Mercator grid obtained from the AVISO website: Archiving, Validation and Interpretation of Satellite Oceanographic Data (http://www.aviso.oceanobs.com/). We calculated the velocities of the geostrophic currents from SLA data as follows:

$$u = -\frac{g}{f}\frac{\partial \zeta}{\partial y}, \quad v = \frac{g}{f}\frac{\partial \zeta}{\partial x} \quad , \tag{2}$$

where g is the acceleration due to gravity (980 cm s^{-2}), f is the Coriolis parameter ($2\Omega \sin \Phi$), Ω is the Earth's angular velocity (7.29 $\times$ 10^{-5} radians per second), Φ is the latitude, $\partial\zeta / \partial y$ and $\partial\zeta / \partial x$ are the north-south and east-west gradients of SLA, respectively. We compared the Chl-*a* concentration images with the geostrophic current images to examine the relationship between phytoplankton distribution and the

geostrophic current.

2.4. Light conditions and stability of the water column

We applied Sverdrup's critical depth theory to understand the timing of the spring bloom. The production of organic matter by photosynthesis cannot exceed the destruction by community respiration, unless a critical depth (CRD) where the integrated production balances the integrated destruction within the water column is shallower than the mixed layer depth (MLD) (Sverdrup, 1953). That is because the phytoplankton are about evenly distributed within a well-mixed layer, while net production takes place only above the compensation depth (i.e., in the euphotic zone). Below the compensation depth there is net loss of phytoplankton due to low irradiance. Thus, if mixing is deeper than the critical depth, the total population of phytoplankton within a water column cannot increase. It is important to compare the CRD with MLD for understanding the variations of phytoplankton biomass.

According to Sverdrup (1953), CRD is defined by the equation

$$\frac{CRD}{1-\mathrm{e}^{-K_d(\mathrm{PAR})\cdot CRD}} = \frac{I_\mathrm{e}}{K_d(\mathrm{PAR})\cdot \mathrm{I_c}}, \tag{3}$$

where K_d(PAR) is the diffuse attenuation coefficient for the Photosynthetically Available Radiation, $\mathrm{I_c}$ is the compensation light intensity and I_e is the PAR at the sea

surface. We used the 8-day mean PAR data from SeaWiFS as I_e in this study. The incident radiation should be reduced by a factor of 0.5 to allow for the absorption of the longer and shorter wavelengths of light in the first few centimeters of water (Parsons and Takahashi, 1973). The energy (I_c) at the compensation depth is taken to be constant, 2.88 W m^{-2} (Strickland, 1958). K_d(PAR) is derived as follows (Morel et al., 2007):

$$K_d(\mathrm{PAR}) = 0.0665 + 0.874K_d(490) - 0.00121[K_d(490)]^{-1} \quad (4)$$

where we took K_d(490) to be the 8-day mean diffuse attenuation coefficient for downward irradiance at 490 nm from SeaWiFS. The K_d coefficients have been computed for the layer corresponding to the first penetration depth from which 90 % of the emerging signal at 490 nm originates (Gordon and McCluney, 1975). The attenuation of total PAR with depth is nearly always approximate, therefore in a given water body it can generally be characterized by a single value K_d(PAR) (Kirk, 1994).

To calculate the MLD, Argo float data obtained from the Global Ocean Data Assimilation Experiment were used in this study. The number of Argo float data during spring in the study area was very small, with only one float each for 2006 and 2007 that continuously measured conductivity, temperature and depth (CTD) every 10 days. Most of the profiles consist of about 70 levels from 5 to 2000 dbar in depth, with

smaller sampling intervals close to the surface and larger intervals at depth. Data with spikes were excluded from analysis. The MLD was defined as the depth at which the potential density was greater than that at the surface by 0.125 kg m^{-3} (e.g., Levitus, 1982; Ladd and Thompson, 2000; Suga et al., 2004). Then we compared the CRD with MLD. We also calculated the Brunt-Väisälä Frequency (BVF) to investigate the stability of the water column at the Argo float observation site (Millard et al., 1990). That is the frequency at which a vertically displaced parcel will oscillate within a statically stable environment. The BVF = N, is given by

$$N = \sqrt{-\frac{g}{\rho}\frac{d\rho}{dz}}, \quad (5)$$

where g is the acceleration due to gravity, ρ is the density of seawater and z is the depth. Higher values of the BVF indicate stronger stratification.

3. Results

3.1. Validation of satellite Chl-*a* concentration data

SeaWiFS Chl-*a* concentrations were compared with in-situ values along the A-line from A1 to A13 (Fig. 2). Some SeaWiFS data were observed outside of the ±35 % line; however, the correlation between SeaWiFS and *in-situ* values was statistically significant with a high coefficient of determination (n = 46, r^2 = 0.90, p <

0.0001). This relationship indicates that Chl-*a* concentration data from SeaWiFS are useful in this study area.

3.2. Chl-*a* seasonality for 10 years from 1998 to 2007

Monthly mean Chl-*a* concentrations during the 10 years from 1998 to 2007 were composited for each calendar month (Fig. 3). In almost the whole region, Chl-*a* concentration was highest during spring each year. It decreased in summer and increased again in autumn. Especially in the east Hokkaido coastal region, large seasonal variability of Chl-*a* concentration was observed, with high values (> 3 mg m^{-3}) occurring during spring. From the analysis of 8-day mean Chl-*a* concentrations averaged in the Oyashio region, it is clear that Chl-*a* concentration was higher than 1.5 mg m^{-3} from early April to early June (i.e., spring bloom), and the interannual variability was substantial from late March to June (Fig. 4). The seasonal cycles of Chl-*a* concentration from March to June in all years of the study are shown in Fig. 5. Quite a high Chl-*a* concentration, 4.7 mg m^{-3}, was observed suddenly in mid-April 1998. At that time the areas indicating Chl-*a* concentrations over 10 mg m^{-3} extended widely along the edge of a cyclonic eddy (not shown). However the high Chl-*a* concentration decreased dramatically, to 1.6 mg m^{-3}, in early May. Early blooms were

observed in early April 2001 (2.3 mg m^{-3}) and late March 2002 (2.1 mg m^{-3}). In 2001 Chl-*a* concentration gradually increased to 3.4 mg m^{-3}, persisting until late April, suggesting that a long and copious spring bloom occurred in that year. Relatively late blooms were observed starting in mid-May 1999 (2.5 mg m^{-3}) and late April 2006 (2.3 mg m^{-3}). The 1999 bloom continued for about one month. The 2006 bloom terminated in mid-May; however, a second bloom was observed from late May to early June (2.9 mg m^{-3}). A late bloom was also observed in early June 2004.

We examined the temporal variation of Chl-*a* concentration during spring using 10-year means of monthly Chl-*a* concentration data. We focused on the highly productive season and then classified areas in the Oyashio region based on the temporal variation pattern of Chl-*a* concentration from March to June. The region was clustered into 3 classes by the ISODATA analysis (Fig. 6). The areas of classes 1 and 2 were mostly distributed to the east and west, respectively, of 148.5 ˚E, (Fig. 6a). The area of class 3 was the coastal waters east of Hokkaido. Chl-*a* concentration in the area of class 1 gradually increased from March (0.34 mg m^{-3}) to June (1.28 mg m^{-3}) (Fig. 6b). Chl-*a* concentrations in the area of classes 2 and 3 were highest in May (2.11 mg m^{-3}) and April (5.21 mg m^{-3}), respectively. Thus, Chl-*a* concentration near the coast off Hokkaido was the highest, and timing of the peak was earlier than in the offshore

region.

3.3. Variability in Chl-*a* concentration along the A-line during spring

We examined the variability in spring bloom along the A-line from 1998 to 2007 (Fig. 7). The variation of Chl-*a* concentration along the A-line during spring indicated large inter-annual variability at each station (Fig. 7a). In the coastal region from A1 to A3, the spring bloom (> 1.5 mg m^{-3}) occurred from April or May and continued until mid- or late June every year (Fig. 7b). However, an extended spring bloom (> 3.0 mg m^{-3} for over 24 days in the region from A1 to A3) did not occur every year but only in 1998, 2001, 2002 and 2007, years in which relatively early blooms (from late March or early April) were observed from A1 to A3 (Fig. 7a and b). On the other hand, relatively short (24 days total days of bloom) and late (mid-April or mid-May) spring blooms were observed in 1999 and 2000. Especially the spring bloom in 2000 was the least extended in the coastal region during 10 years.

Spring blooms were also observed in the offshore region from A4 to A13 (Fig. 7b). However, they tended to be smaller, shorter and later than those in the coastal region. The high Chl-*a* concentration area extended from the coast to offshore waters (Fig. 8a). From time-series of Chl-*a* concentration images, high Chl-*a* concentrations

around the coastal region progressively extended offshore (Fig. 9a). In these high Chl-*a* areas, mesoscale eddies or strong currents often appear in the images of geostrophic currents (Fig. 8b). Cyclonic eddies were present in the flow offshore to the east of Hokkaido, centered around 146 ˚E, in 1998, 1999, 2000, 2001 and 2004. Along the edges of these cyclonic eddies high Chl-*a* concentrations were clearly observed (Fig. 8a and b). High Chl-*a* concentration areas were also distributed along currents with relatively high velocity (> 10 cm s^{-1}) in 2002, 2005. Fig. 9 indicates that Chl-*a* concentration increased more strongly in the area receiving currents from the coastal region. At station A5 (42 ˚N, 145.25 ˚E), where the Oceanic Ecodynamics Comparison in the Subarctic Pacific (OECOS) cruises from Japan were conducted during March 8 to 15 and April 5 to May 1, 2007, a spring bloom occurred in that year from early April (Fig. 7b), and southward currents were observed from an area of high Chl-*a* concentration (Fig. 8a and b). A mesoscale eddy was observed around A5 from mid-April and Chl-*a* concentration was relatively high (> 3 mg m^{-3}) around the eddy in late April (Fig. 9).

3.4. Spatial and temporal variability in Chl-*a* concentration and environmental condition of the water column

Fig. 10 presents the spatio-temporal variability of Chl-*a* concentration in the Oyashio region, not only along the A-line, from 1998 to 2007. The variation patterns of Chl-*a* concentration in each clustered area were obviously different between years. Spatio-temporal variability in Chl-*a* concentration during spring is strong in the Oyashio region. We examined the variation pattern of Chl-*a* concentration in each region and in each year. It was observed that in the coastal region off Hokkaido the spring bloom generally occurred in April and Chl-*a* concentration was higher than in the region off the Kuril Islands or in the offshore region. In 2001, 2002 and 2006, the area where Chl-*a* concentration was highest in April was more extensive than usual, whereas it was narrowly distributed in 2003. In 1999 the area where Chl-*a* concentration was highest in May was the widest among the 10 years, which was linked to the relatively late occurrence of the bloom in that year (Fig. 5). In 2004, the spring bloom strengthened off Hokkaido until May and in some areas it occurred in June, which was also linked to the overall delay of the bloom shown in Fig. 5. Off Hokkaido in 2000, the spring bloom area was more narrowly confined near the coast than usual. The temporal pattern of Chl-*a* concentration increasing from March to June was prominent in 2001, 2004, 2005, 2006 and 2007 (Fig. 10). However, that pattern was not prominent every year. It is clear that the variation of Chl-*a* concentration along

the A-line differed among years.

Each Argo float in 2006 and 2007 measured conductivity, temperature and depth within one clustered area (Fig. 10a). When the MLD became shallower than the CRD in early April 2006 and late April 2007, Chl-*a* concentration increased from 0.8 to 2.4 mg m^{-3} and from 0.35 to 0.63 mg m^{-3}, respectively (Fig. 11a). Simultaneously, less dense water (less saline or warmer water) than in the previous observation was observed in the surface layer (not shown), resulting in a relatively high BVF (> 0.01 s^{-1}) in the upper layer, indicating a stratified water column (Fig. 11b). During the bloom onsets in 2006 and 2007 the MLDs were almost the same, 94 and 99 m depth, relatively. The BVF in 2006 was larger than in 2007. Later in the season, the MLDs were shallower, < 10 m by late June in both 2006 and 2007, and Chl-*a* concentration eventually decreased to 0.63 and 0.39 mg m^{-3}, respectively.

4. Discussion

The spring bloom occurs in the Oyashio region every year; however, its magnitude, duration and timing are substantially different among areas and years. Usually the termination of the spring bloom corresponds with the depletion of macronutrients (Kudo et al., 2000). On the other hand, Saito et al. (2002) have

suggested that its termination is not always dependent on macronutrient depletion, that the magnitude and duration of bloom in the Oyashio region may be controlled by grazing pressure from zooplankton. Of course, grazing does not prevent the initiation of the bloom, however, the inter-annual variability of the magnitude and duration of the spring bloom, shown in Fig. 5 and Fig. 7, might result from the inter-annual variability of zooplankton grazing. However, it is difficult to consider the mechanisms of the spring bloom along the A-line being the same as those in the Oyashio as a whole, because the spatio-temporal variability in Chl-*a* concentration clearly differs across the region, particularly between the coastal waters east of Hokkaido and the oceanic region (Fig. 7 and Fig. 10). Some stations where nutrients were depleted in April or May have been observed along the A-line in the years from 1990 to 1998 (Saito et al., 2002, Fig. 2). This suggests that the termination of the spring bloom is quite possibly affected by nutrient depletion. The characteristics of water masses can also differ among areas and years because of the complexity of geostrophic currents that advect water from different sources (Fig. 7b).

The initiation of the spring bloom in the Oyashio region has been explained by Sverdrup's critical depth theory (e.g., Yoshimori et al., 1995). In this study Chl-*a* concentration also increased rapidly when the MLD was shallower than the CRD (Fig.

11). MLD is not the only important aspect of water column stability. MLDs in 2006 and 2007 were almost the same, but the BVFs in were greater 2006 than in 2007, and the strong stratification may be a reason for the higher Chl-*a* concentrations in 2006. The stratification caused by less dense water (Fig. 11) can result from the transport of the coastal water with low salinity. No spring bloom was observed at Argo float positions in 2007 (i.e., Chl-*a* was < 1.5 mg m^{-3}); however, Chl-*a* concentration nearly doubled, which was explained by Sverdrup's critical depth theory (Fig. 11a). After that, Chl-*a* concentration decreased and the spring bloom terminated due to zooplankton grazing or nutrient depletion by strengthened stratification (Fig. 11). Although this result lacks quantitative and statistical rigor, due to the paucity of Argo data in the Oyashio region, it supports Sverdrup's critical depth theory for this region in a general way.

As shown in Fig. 10, the spatio-temporal variability of Chl-*a* concentration during spring was strong in the Oyashio region, and Chl-*a* concentration was high, especially in the coastal area. The Coastal Oyashio Water (COW), low salinity, less dense water, often is carried southwestward along the continental slope southeast of Hokkaido by the Oyashio (Kono et al., 2004). It carries dense phytoplankton stocks and strong stratification out into the oceanic extension of the Oyashio. The mesoscale

eddies east of Hokkaido, or southward currents from the coastal region, would also transport the COW with high Chl-*a* concentration during spring (Fig. 8 and Fig. 9). If the current speed at the edge of a mesoscale eddy is 50 cm s^{-1}, the COW will be transported to 3.2 degrees (345.6 km) away in 8 days. In the area to which the COW was transported, stratification would be enhanced in the surface layer, causing further increase in Chl-*a* concentration. Satellite ocean color images show that Chl-*a* concentration increased more strongly in the area receiving currents from the coastal region (Fig. 9).

The variation pattern of Chl-*a* concentration during spring can be determined by geostrophic currents such as mesoscale eddies, which would be one of the reasons for the spatio-temporal variability in Fig. 10. However, to verify the theory about the enhancement of stratification by the propagation of COW, further ship or float observation data will be necessary, simultaneous with satellite data. The analysis and consideration of geostrophic currents will enable us to discuss the variability of spring blooms with greater spatial and temporal precision.

Acknowledgments

This study was conducted as part of Oceanic Ecodynamics Comparison in the

Subarctic Pacific (OECOS) project. We thank Mrs. Amane Fujiwara and Shintaro Takao, students in Hokkaido University, for their valuable discussions. We also appreciate three anonymous reviewers for their constructive comments. Ocean color data used in this study were produced by the SeaWiFS Project at the NASA Goddard Space Flight Center. Sea surface height anomaly data were produced by the Archiving, Validation and Interpretation of Satellite Oceanographic Data scientific team of Collecte, Localisation, Satellite, Centre National d'Etudes Spatiales data center. This study was supported by funds from Ministry of Education, Culture, Sports, Science and Technology, Japan, a Grant-in-Aid for Scientific Research in Priority Areas: "Western Pacific Air-Sea Interaction Study (W-PASS)" under Grant No.18067003. This study is a contribution to the Surface Ocean Lower Atmosphere Study (SOLAS) Core Project of the International Geosphere-Biosphere Programme (IGBP).

References

Carder, K.L., Steward, R.G., Harvey, G.R., Ortner, P.B., 1989. Marine humic and fulvic acids: Their effects on remote sensing of ocean chlorophyll. Limnology and Oceanography 34, 68-81.

Chiba S., Ono, T., Tadokoro, K., Midorikawa, T., Saino, T., 2004. Increased stratification and decreased lower trophic level productivity in the Oyashio region of the North Pacific: A 30-year retrospective study. Journal of Oceanography 60, 149-162.

ERDAS, 1999. ERDAS Field Guide, Fifth edition, ERDAS, Atlanta, GA, 698pp.

FRA, 2009. A-line data home page, http://hnf.fra.affrc.go.jp/a-line/.

Gordon, H.R., McCluney, W.R., 1975. Estimation of the depth of sunlight penetration in the sea for remote sensing. Applied Optics 14, 413-416.

Kasai, H., Saito, H., Yoshimori, A., Taguchi, S., 1997. Variability in timing and magnitude of spring bloom in the Oyashio region, the western subarctic Pacific off Hokkaido, Japan. Fisheries Oceanography 6, 118-129.

Kasai, H., Ono, T., 2007. Has the 1998 regime shift also occurred in the oceanographic conditions and lower trophic ecosystem of the Oyashio region? Journal of Oceanography 63, 661-669.

Kirk, J.T.O., 1994. Light and photosynthesis in aquatic ecosystems. Cambridge University Press, Cambridge, 528pp.

Kono, T., 1997. Modification of the Oyashio Water in the Hokkaido and Tohoku areas. Deep-Sea Research I 44, 669-688.

Kono, T., Foreman, M., Chandler, P., Kashiwai, M., 2004. Coastal Oyashio South of Hokkaido, Japan. Journal of Physical Oceanography 34, 1477-1494.

Kudo, I., Yoshimura, T., Yanada, M., Matsunaga, K., 2000. Exhaustion of nitrate terminates a phytoplankton bloom in Funka Bay, Japan: Change in SiO_4:NO_3 consumption rate during the bloom. Marine Ecology Progress Series 193, 45-51.

Ladd, C., Thompson, L., 2000. Formation mechanisms for North Pacific Central and Eastern Subtropical Mode Waters. Journal of Physical Oceanography 30, 868-887.

Lee, Z., Carder, K.L., Hawes, S.K., Steward, R.G., Peacock, T.G., Davis, C.O., 1994. Model for the interpretation of hyperspectral remote-sensing reflectance. Applied Optics 33, 5721-5732.

Levitus, S., 1982. Climatological atlas of the world ocean. NOAA Professional Paper 13, 173pp.

Millard, R.C., Owens, W.B., Fofonoff, N.P., 1990. On the calculation of the Brunt-Väisälä frequency. Deep-Sea Research 37A, 167-181.

Morel, A., Huot, Y., Gentili, B., Werdell, P.J., Hooker, S.B., Franz, B.A., 2007. Examining the consistency of products derived from various ocean color sensors in open ocean (Case 1) waters in the perspective of a multi-sensor approach. Remote Sensing of Environment 111, 69-88.

Nishioka, J., Ono, T., Saito, H., Nakatsuka, T., Takeda, S., Yoshimura, T., Suzuki, K., Kuma, K., Nakabayashi, S., Tsumune, D., Mitsudera, H., Johnson, W.K., Tsuda, A., 2007. Iron supply tothe western subarctic Pacific: Importance of iron export from the Sea of Okhotsk. Journal of Geophysical Research 112, C10012, doi:10.1029/2006JC004055.

O'Reilly, J.E., Maritorea, S., Mitchell, B.G., Siegel, D.A., Carder, K.L., Garver, S.A., Kahru, M., McClain, C., 1998. Ocean color chlorophyll algorithms for SeaWiFS. Journal of Geophysical Research 103 (C11), 24937-24953.

O'Reilly, J.E., Maritorea, S., O'Brien, M.C., Siegel, D.A., Toole, D., Menziers, D., Smith, R.C., Mueller, J.L., Mitchell, B.G., Kahru, M., Chavez, F.P., Strutton, P., Cota, G.F., Hooker, S.B., McClain, C.R., Carder, K.L., Muller-Karger, F., Harding, L., Magnuson, A., Phinney, D., Moore, G.F., Aiken, J., Arrigo, K.R., Letelier, R., Culver, M., 2000. SeaWiFS Postlaunch Calibration and Validation Analyses, Part 3, SeaWiFS Postlaunch Technical Report Series, Volume 11, NASA Tech. Memo.

2000-206892, S.B. Hooker and E.R. Firestone, Eds., NASA Goddard Space Flight Center, Greenbelt, Maryland.

Parsons, T.R., Takahashi, M., 1973. Biological oceanographic processes. Pergamon Press, Oxford, 196pp.

Saito, H., Tsuda, A., Kasai, H., 2002. Nutrient and plankton dynamics in the Oyashio region of the western subarctic Pacific Ocean. Deep-Sea Research II 49, 5463-5486.

Sakurai, Y., 2007. An overview of the Oyashio ecosystem. Deep-Sea Research II 54, 2526-2542.

Strickland, J.D.H., 1958. Solar radiation penetrating the ocean. A review of requirements, data and methods of measurement, with particular reference to photosynthetic productivity. Journal of the Fisheries Research Board of Canada 15, 453-493.

Suga, T., Motoki, K., Aoki, Y., 2004. The North Pacific climatology of winter mixed layer and mode waters. Journal of Physical Oceanography 34, 3-22.

Sverdrup, H.U., 1953. On conditions for the vernal blooming of phytoplankton. Journal du Conseil Permanent International pour l’Exploration de la Mer 18, 287-295.

Taniguchi, A., 1999. Differences in the structure of the lower trophic levels of pelagic ecosystems in the eastern and western subarctic Pacific. Progress in Oceanography 43, 289-315.

Yoshimori, A., Ishizaka, J., Kono, T., Kasai, H., Saito, H. Kishi, M.J. and Taguchi, S., 1995. Modeling of spring bloom in the western subarctic Pacific (off Japan) with observed vertical density structure. Journal of Oceanography 51, 471-488.

Figure captions

Fig. 1. Schematic illustration of the currents around the Oyashio region and the location of A-line stations A1 (42.83 ˚N, 144.83 ˚E) to A13 (40 ˚N, 146.25 ˚E). The variability of Chl-*a* concentration along this line is depicted in Fig. 5. EKC: East Kamchatka Current, SWC: Soya Warm Current. Dashed box indicates the study area.

Fig. 2. A comparison of the in-situ and SeaWiFS Chl-*a* concentrations along the A-line. The dashed lines delimit the ±35 % range of agreement with respect to the 1:1 line.

Fig. 3. Climatological monthly composites (1998-2007) of Chl-*a* concentration in the Oyashio region. The Sea of Okhotsk was excluded from analysis in this study.

Fig. 4. The seasonal variability of Chl-*a* concentration in the Oyashio region, averaged for 10 years from 1998 to 2007. Gray band indicates the period (from March to June) analyzed in this study.

Fig. 5. Time-series variability of Chl-*a* concentration averaged in the Oyashio region

during spring from 1998 to 2007. The aqua line indicates the 10-year mean data in Fig. 4.

Fig. 6. (a) Spatial distribution of each class of seasonal variation pattern determined by the ISODATA algorithm from 10-years of monthly mean Chl-*a* concentration data from the Oyashio region. The orange line indicates the A-line. (b) Seasonal variability of Chl-*a* concentration in the region of each class.

Fig. 7. (a) Time vs. latitude plots of 8-day mean Chl-*a* concentration along A-line (from A1 to A13). Black boxes indicate no data due to cloud cover. (b) Time vs. latitude plots of the spring bloom along the A-line. Light gray and dark gray boxes indicate Chl-*a* concentrations from 1.5 to 3.0 mg m^{-3} and over 3.0 mg m^{-3}, respectively. Red line indicates the separation between the coastal (A1-A3) and offshore region (A4-A13).

Fig. 8. (a) SeaWiFS images of 8-day mean Chl-*a* concentration during the first or second week of April in each year of the study, and (b) weekly geostrophic currents in approximately the same period as (a).

Fig. 9. (a) SeaWiFS images of 8-day mean Chl-*a* concentration from March 22 to April 30 1998 (left) and 2007 (right) and (b) weekly geostrophic currents in approximately the same periods as (a). The white dots surrounded by black circles indicate the location of A5 (42 ˚N, 142.25 ˚E).

Fig. 10. (a) Spatial distribution of each class determined in the seasonal variation pattern of Chl-*a* concentration in each year from 1998 to 2007. The orange line indicates the A-line. Circles and lines on the clustering maps of 2006 and 2007 indicate the tracks of two Argo floats analyzed in Fig. 11. Red dashed arrows indicate the directions of movement of the Argo floats. Red circles are the positions where the MLD became shallower than the CRD, corresponding to the pink zone in Fig. 11a. (b) Seasonal variability of Chl-*a* concentration in the region of each class.

Fig. 11. (a) Time-series of the MLD variability (blue line), CRD (orange line) and sea surface Chl-*a* concentration (green line). Pink zone in the middle panel indicates the period when the MLD became shallower than the CRD, corresponding to the red circle in Fig. 10a. (b) Time-series variability of the BVF. The MLD and BVF were

calculated from Argo float data. The CRD and Chl-*a* concentration at the Argo float stations were derived from satellite data.

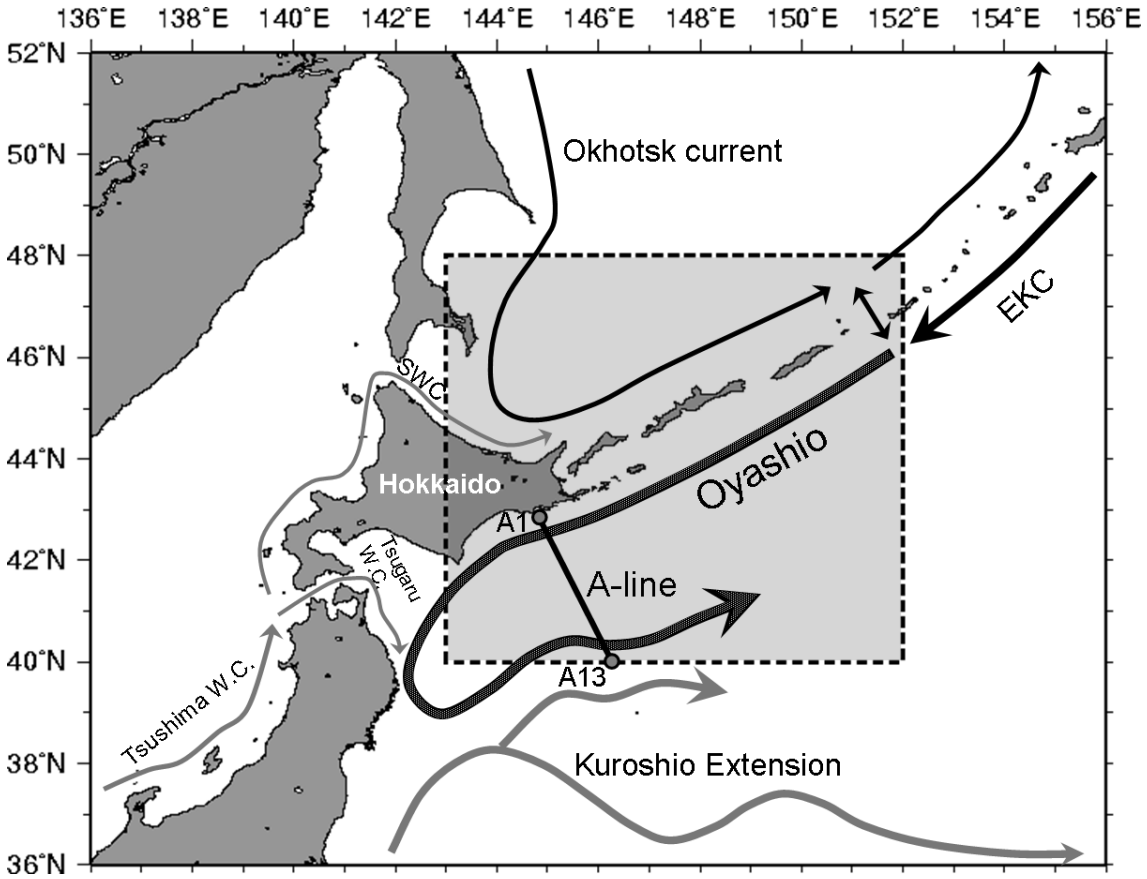

Fig. 1

Okamoto, Hirawake and Saitoh

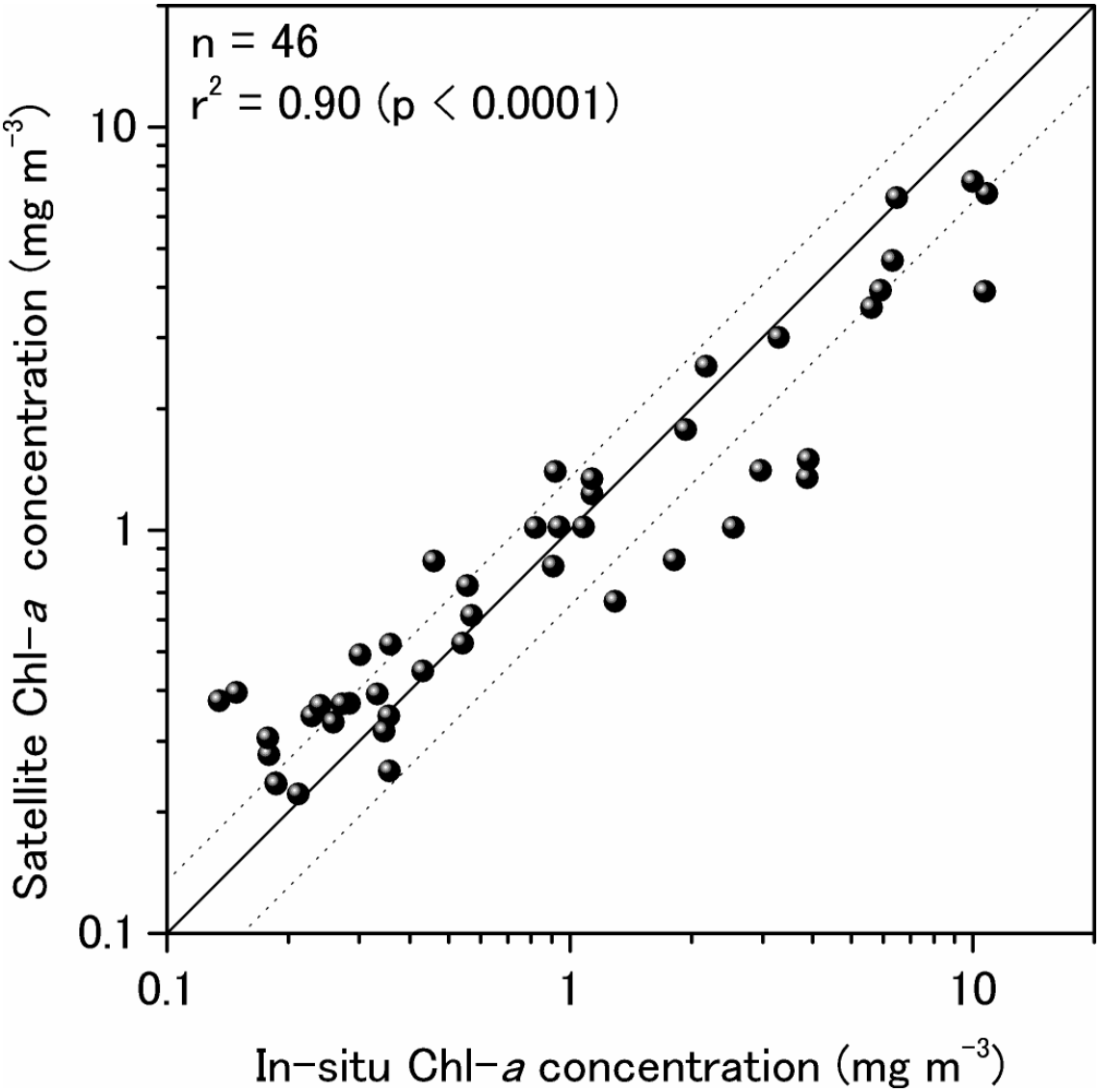

Fig. 2

Okamoto, Hirawake and Saitoh

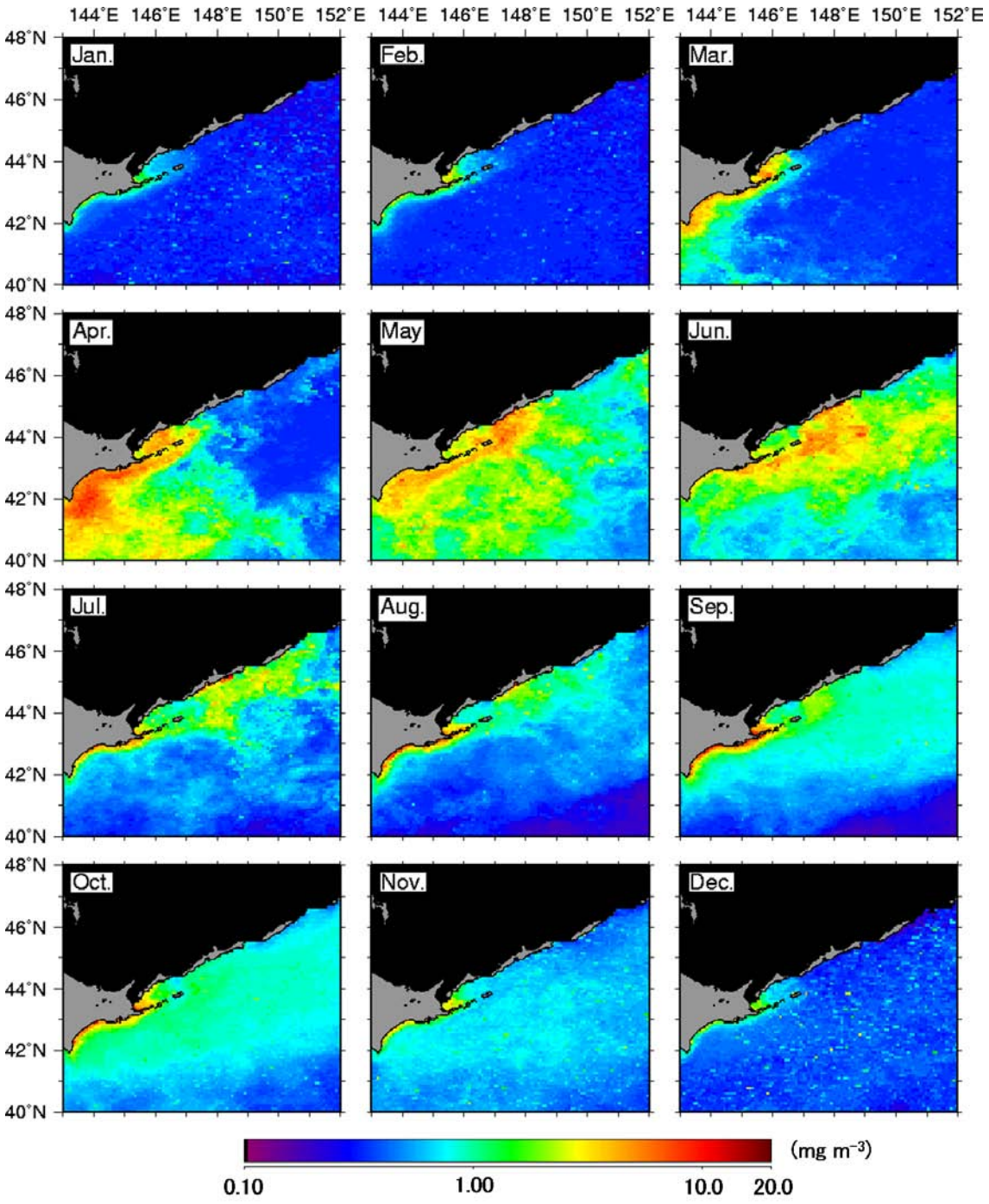

Fig. 3

Okamoto, Hirawake and Saitoh

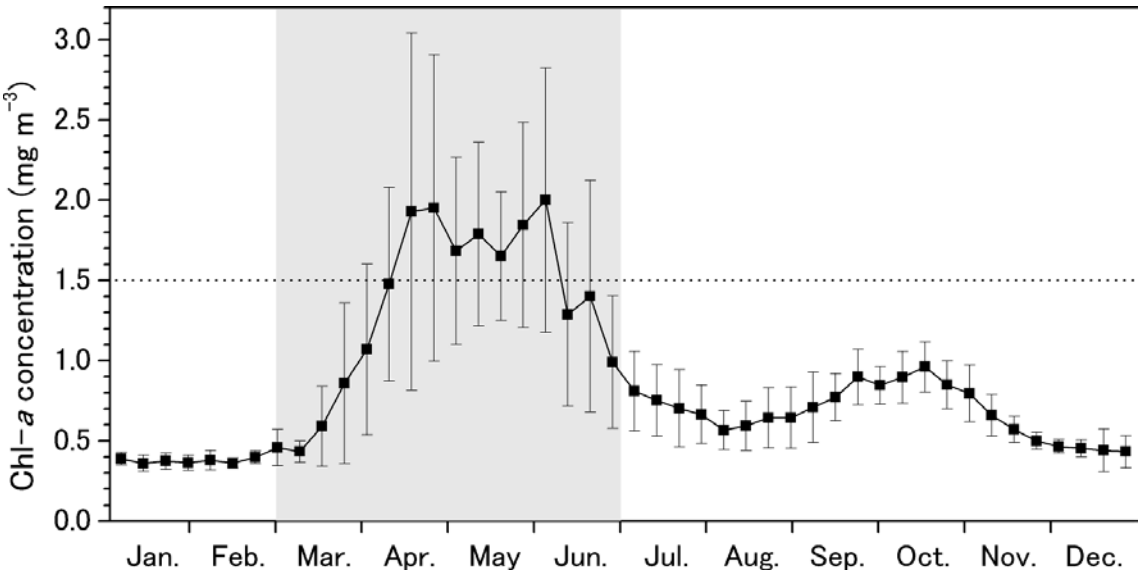

Fig. 4

Okamoto, Hirawake and Saitoh

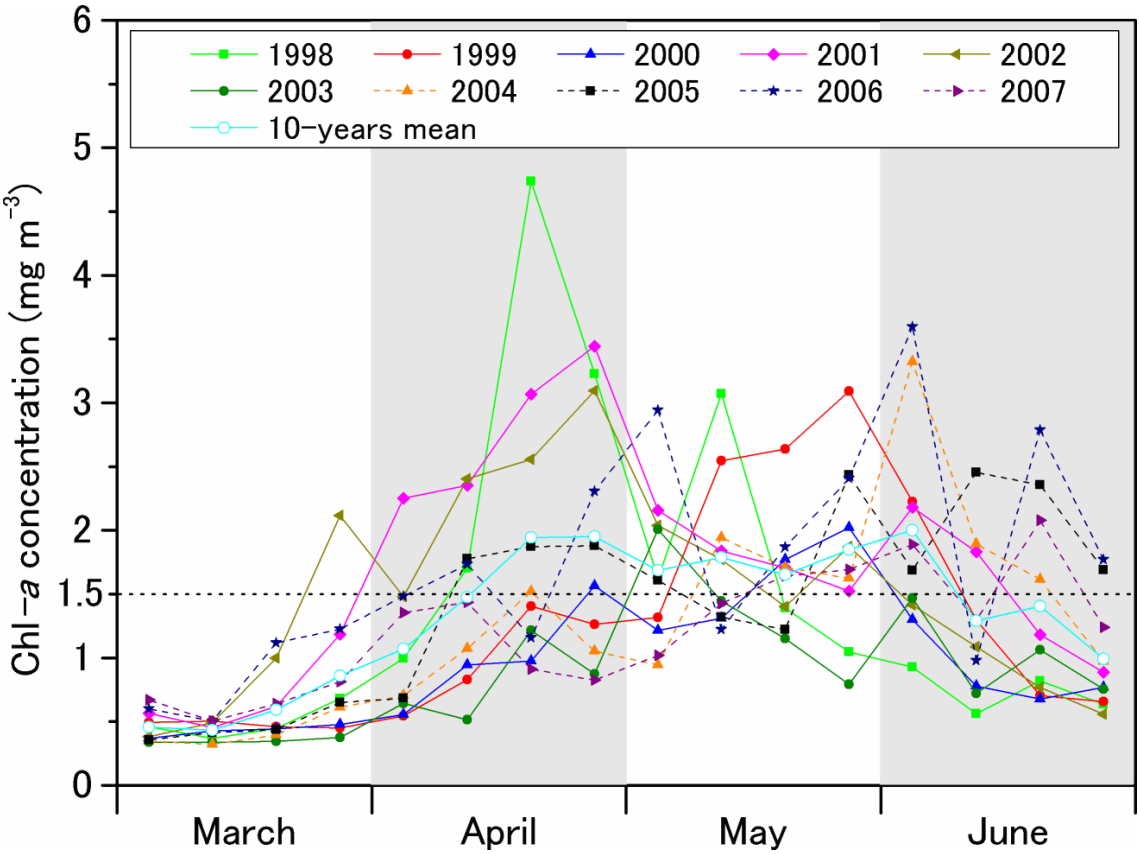

Fig. 5

Okamoto, Hirawake and Saitoh

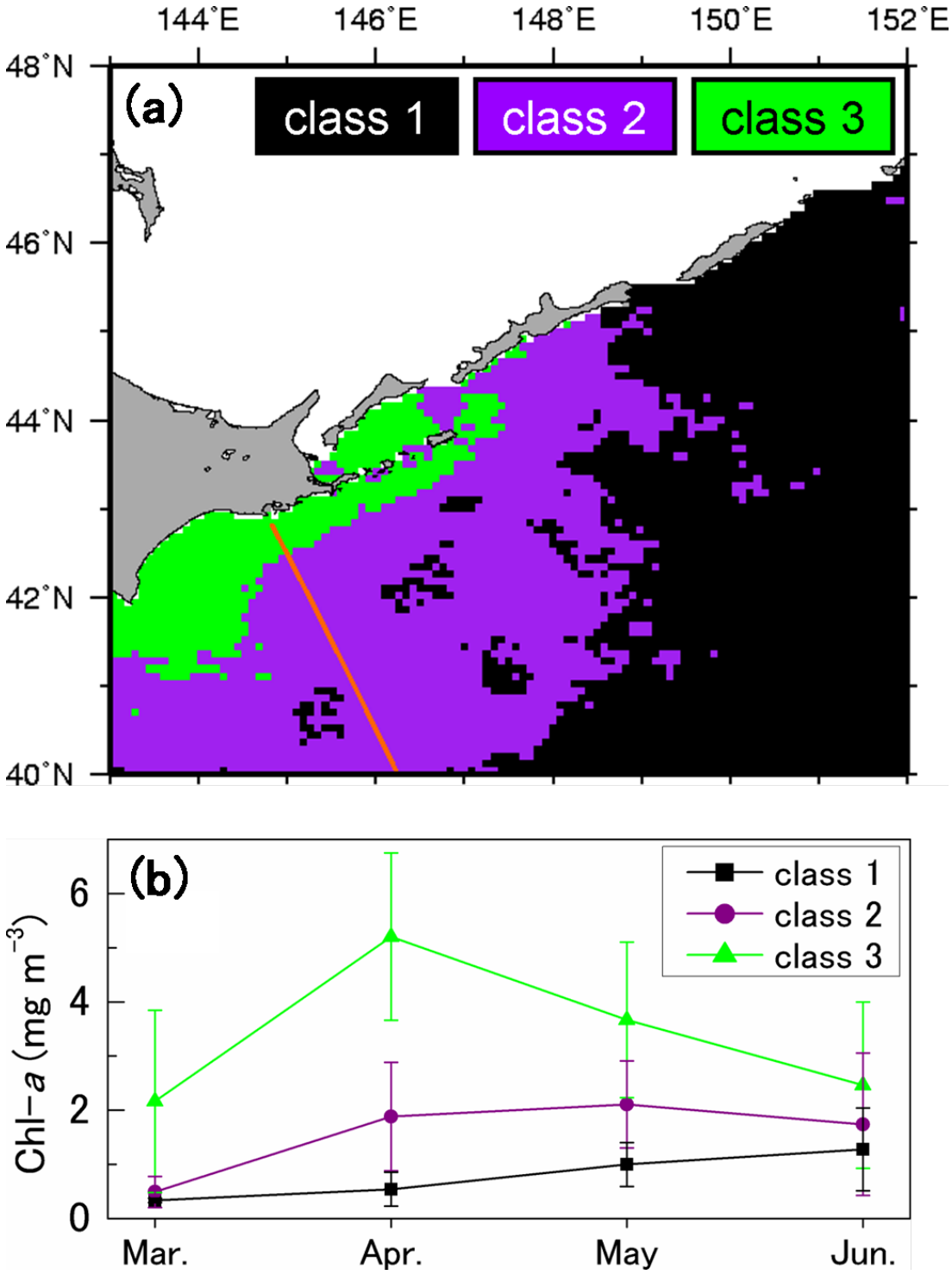

Fig. 6

Okamoto, Hirawake and Saitoh

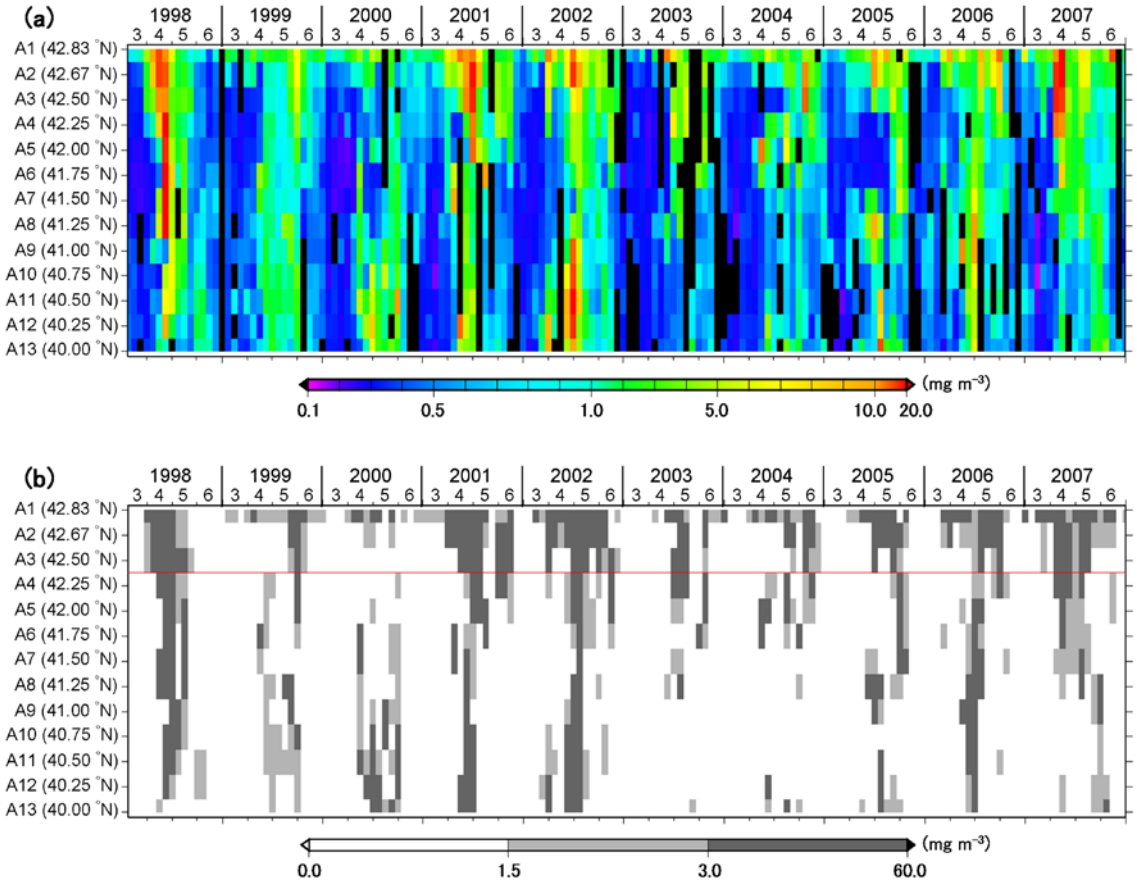

Fig. 7

Okamoto, Hirawake and Saitoh

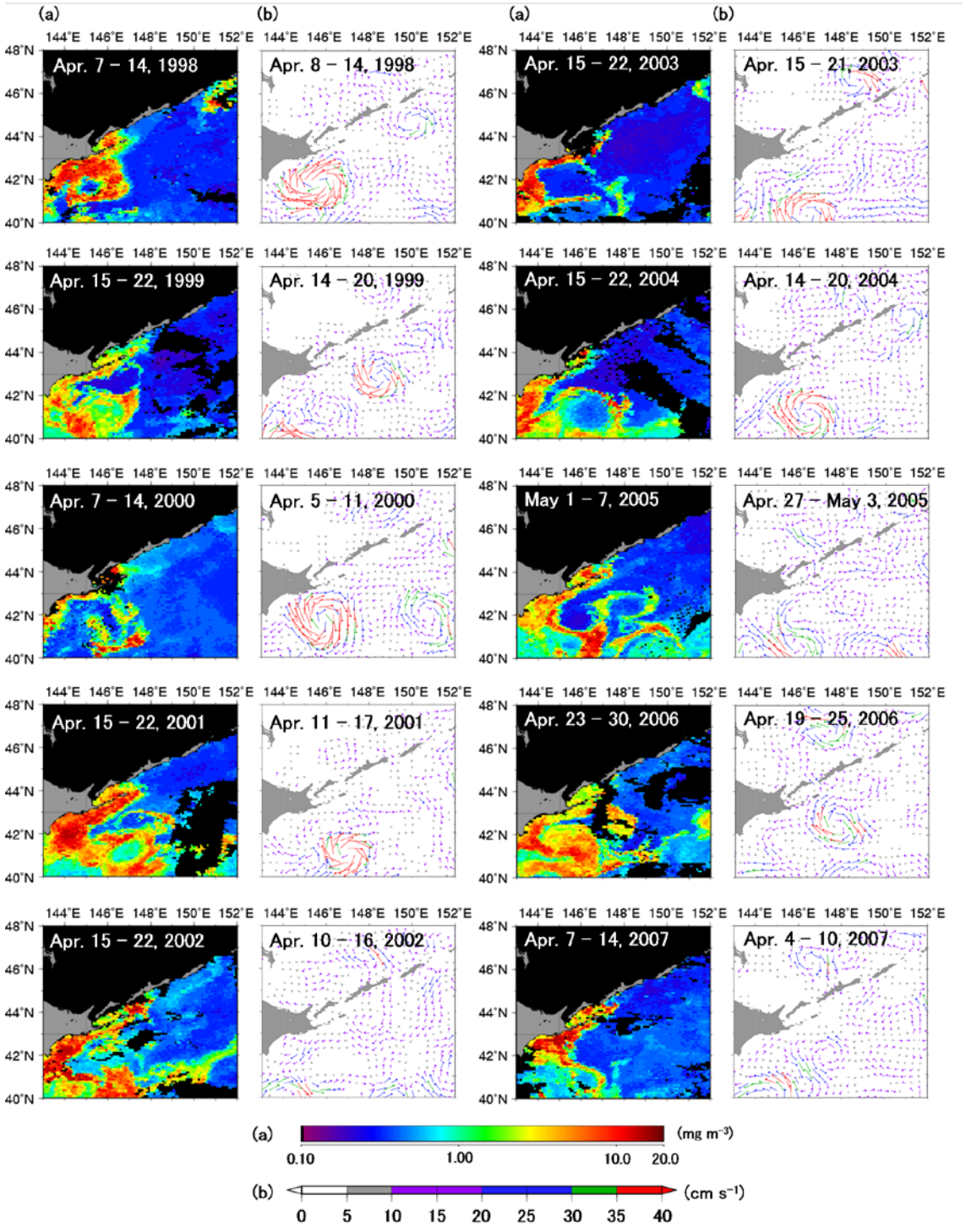

Fig. 8

Okamoto, Hirawake and Saitoh

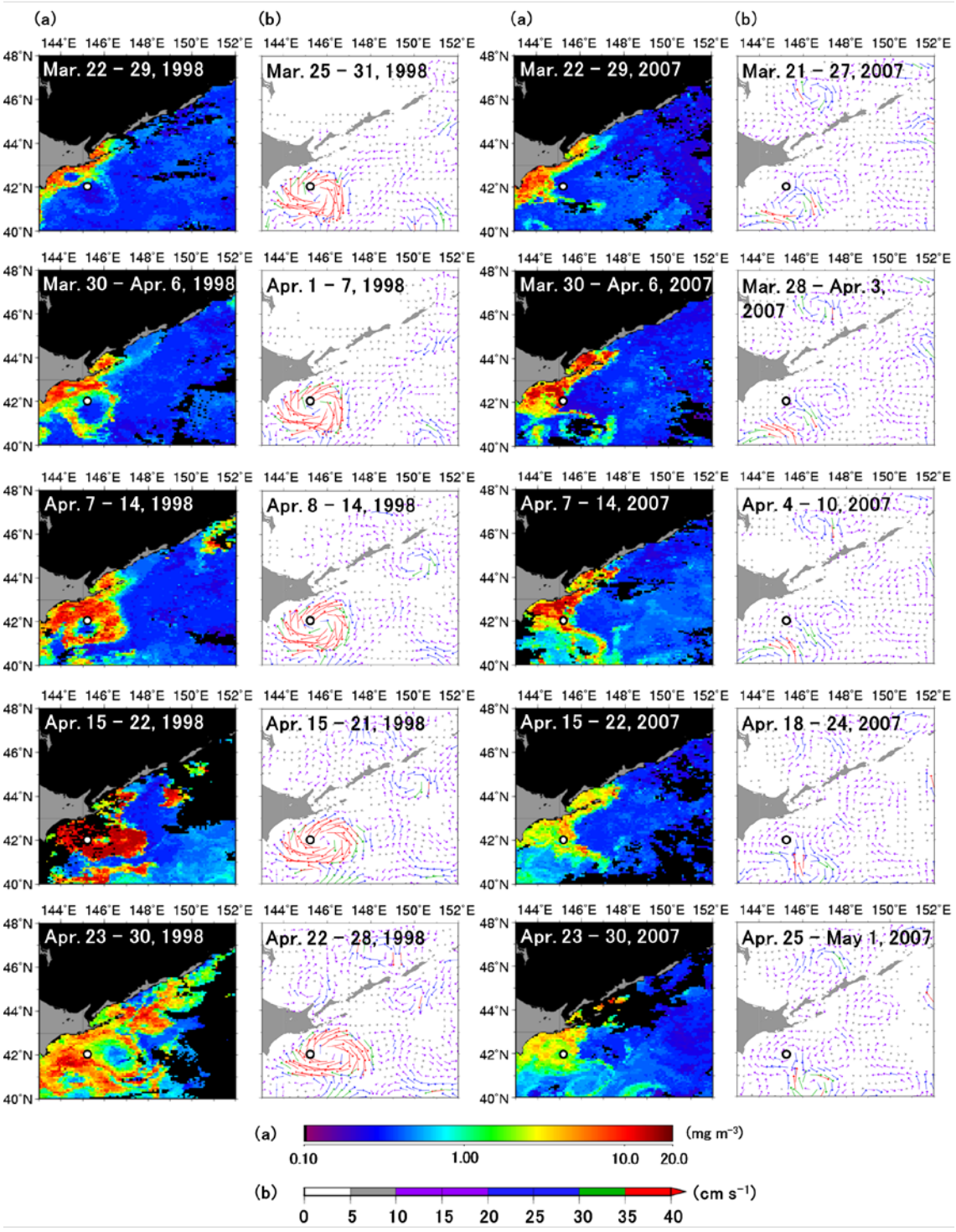

Fig. 9

Okamoto, Hirawake and Saitoh

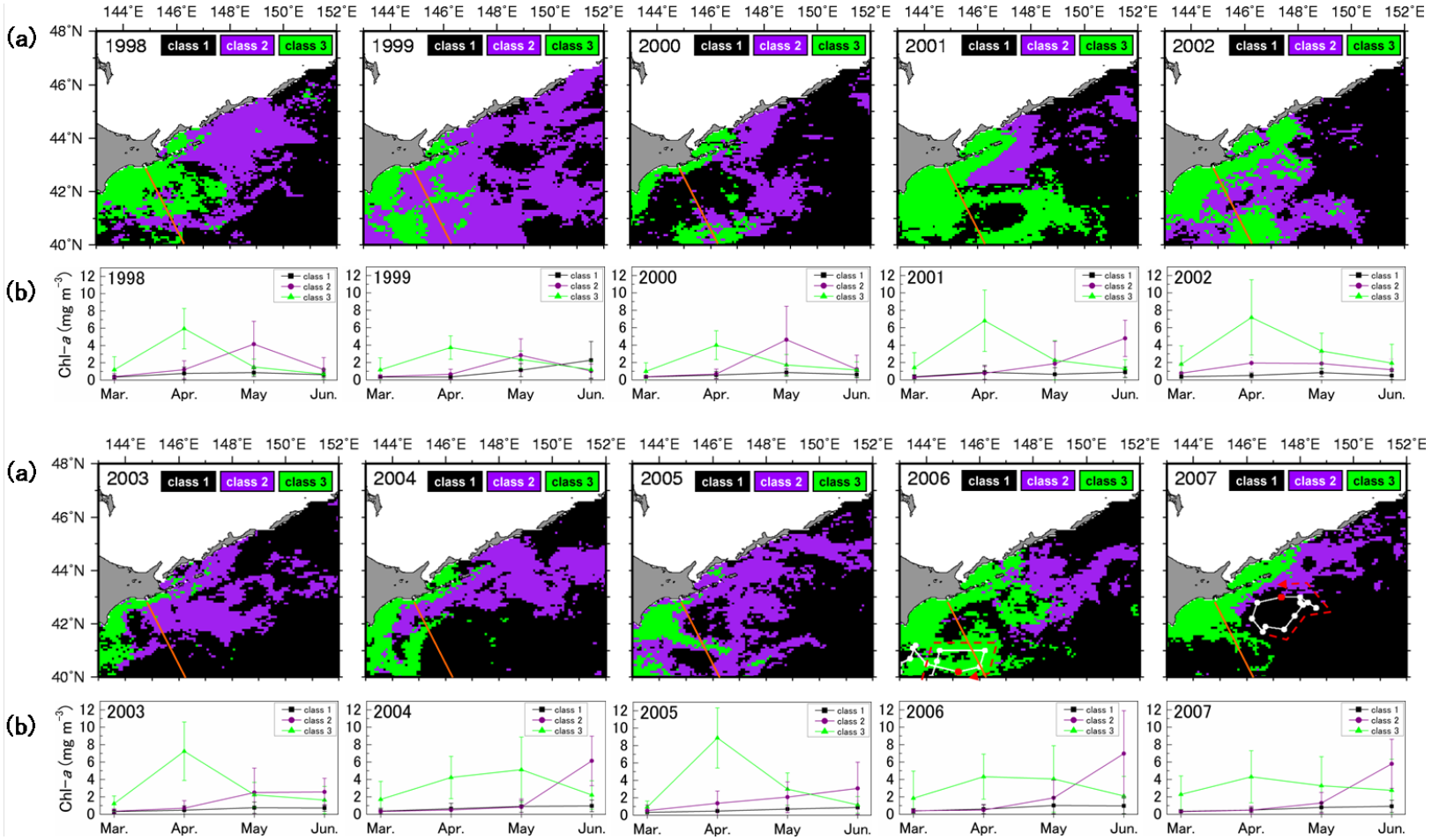

Fig. 10

Okamoto, Hirawake and Saitoh

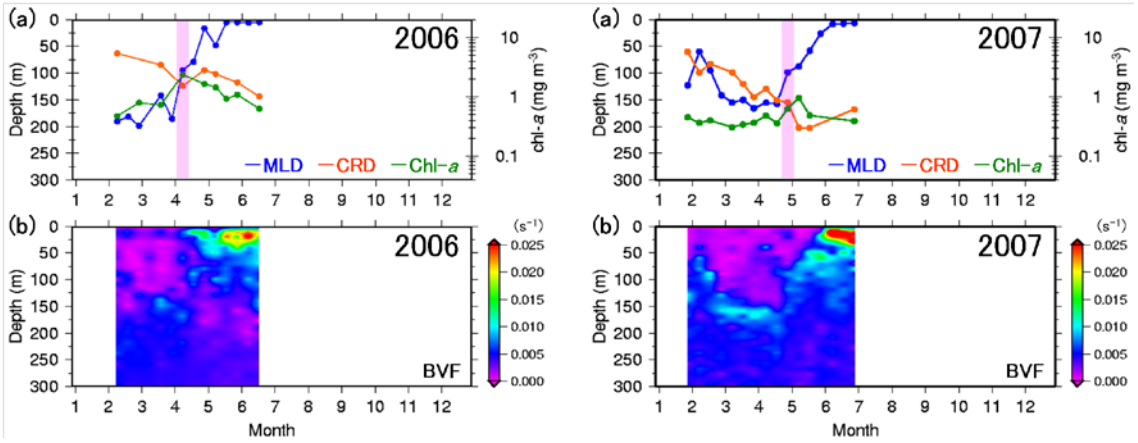

Fig. 11

Okamoto, Hirawake and Saitoh